CH-99-8-2 (RP-899)

# Large-Scale Physical Model Studies for an Atrium Smoke Exhaust System

**Gary D. Lougheed, Ph.D.**
*Member ASHRAE*

**George V. Hadjisophocleous, Ph.D., P.Eng.**

**Cameron McCartney**

**Bruce C. Taber**

## ABSTRACT

*This paper presents results of a project initiated by ASHRAE and the National Research Council of Canada. The project applies both physical and numerical modeling to atrium smoke exhaust systems to investigate the effectiveness of such systems and to develop guidelines for their design.*

*In this paper, results were obtained from a series of tests conducted using a large-scale physical model. The results from the physical model studies are used to investigate the effect of various parameters including fire size, volumetric flow rate for the smoke exhaust system, and the number and location of the exhaust inlets on the conditions in the atrium.*

## INTRODUCTION

An atrium within a building is a large open space created by an opening, or series of openings, in floor assemblies, thus connecting two or more stories of a building.[1] This design feature has gained considerable popularity, mainly because of its visual appeal. The sides of an atrium may be open to all floors, open to some of the floors, or closed to all or some of the floors by unrated or rated fire-resistant construction. Also, there may be two or more atria within a single building, all interconnected at the ground floor or on a number of floors.

By interconnecting floor spaces, an atrium violates the concept of floor-to-floor compartmentation, which is intended to limit the spread of fire and smoke from the floor of fire origin to other stories inside a building. With a fire on the floor of an atrium or in any space open to it, smoke can fill the atrium and connected floor spaces. Elevators, open stairs, and egress routes that are within the atrium space can also become smoke laden.

Protecting the occupants of a building from the adverse effects of smoke in the event of a fire is one of the primary objectives of any fire protection system design. Achieving this objective becomes more difficult when dealing with very large spaces, such as an atrium or an indoor sports arena, where a large number of occupants may be present and the compartment geometries may be complex. Because of these difficulties, model building codes place restrictions on the use of atrium spaces in buildings. Some of the requirements, which are commonly applied in codes for buildings with atria, include:

- the installation of automatic sprinklers throughout the building,
- limits on combustible materials on the floor of an atrium,
- the installation of mechanical exhaust systems for use by firefighters, and
- the provision of smoke management systems to maintain tenable conditions in egress routes.

Atrium smoke management systems have become common in recent years, and design information for these systems is provided by NFPA 92B (NFPA 1995) and Klote and

1. For the purposes of this paper, the definition of "atrium" will be in accordance with that used in NFPA 92B (1995) and by Klote and Milke (1992), that is, a large volume space in a commercial building. This includes office buildings, hotels, and hospitals with typical atrium spaces, covered malls, and other buildings with similar large volume spaces. It does not include warehouses, manufacturing facilities, or other similar spaces with high fire load densities.

**Gary D. Lougheed** and **George V. Hadjisophocleous** are senior research officers and **Cameron McCartney** and **Bruce C. Taber** are technical officers at the National Research Council of Canada, Ottawa, Ontario.

where

$T_{max}$ = the maximum temperature,

$T_b$ = the temperature near the bottom of the compartment.

In the references, the interpolation constant, $C_n$, was typically assumed to be in the range of 0.15 to 0.2. By using a low value for $C_n$, the smoke interface height is estimated to be near the base of the transition zone between the hot and cold layers. For life safety purposes, this gives a conservative estimate for the height of the smoke interface.

A similar interpolation process was used to analyze the experimental and numerical temperature and $CO_2$ profiles to determine the smoke interface heights. However, since a number of the calculations given in engineering design guides such as NFPA 92B (NFPA 1995) are based on the location of the bottom of the hot zone (top of the transition zone), estimates for the top and bottom of the transition zone are provided.

## LARGE-SCALE PHYSICAL MODEL STUDIES

### Test Facility

A large-scale test facility was constructed in one corner of a hall, which has a clear height of 12.2 m. All dimensions for this facility were approximately two times the small-scale test facility described in Lougheed and Hadjisophocleous (1997). Plan and elevation drawings for the large-scale test arrangement are shown in Figures 1 and 2, respectively.

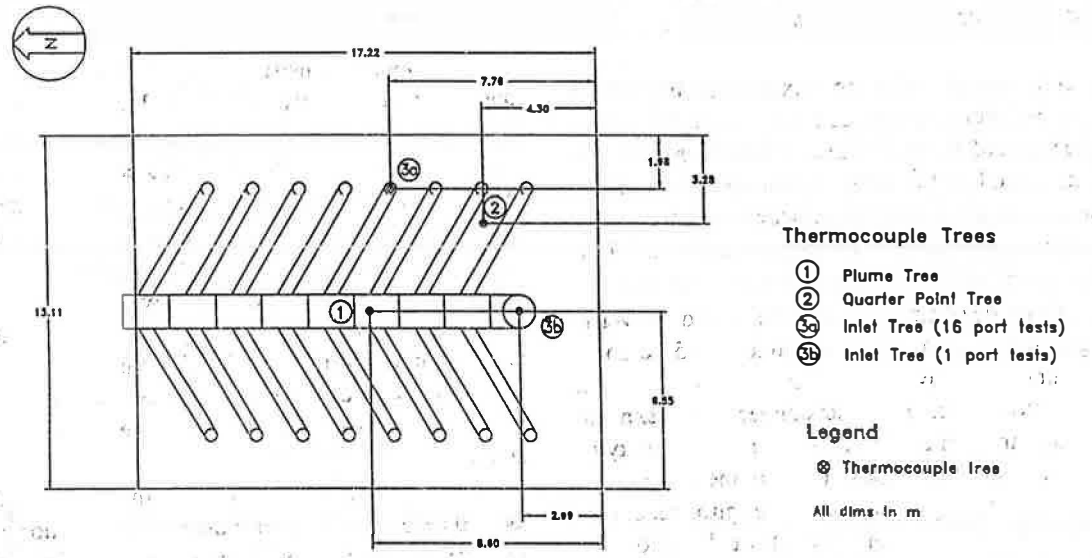


***Figure 1*** *Large-scale atrium facility and instrumentation (plan).*

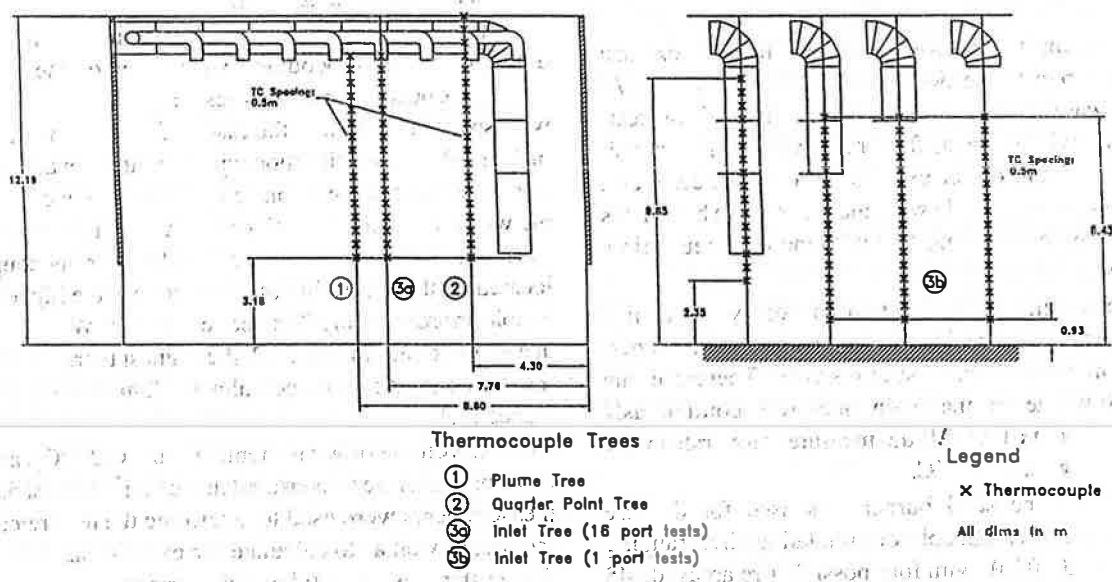


***Figure 2*** *Large-scale atrium facility and instrumentation (elevation).*

The large-scale facility was approximately 13.1 m × 17.2 m. Two sides of the facility were the exterior walls of the hall. The other two sides were formed using draft curtains constructed using solid glass fiber insulation mounted in a lightweight steel frame. The steel frame was attached to cables connected to the ceiling and floor of the hall and spaced at 4 m intervals. The lower 3 m of the interior partitions were left open to the main hall facility to provide ventilation to the test area.

A 1.2 m diameter duct was attached below the ceiling of the atrium test facility, as shown in Figures 1 and 2. This duct entered the test facility through the north interior partition. For one test arrangement, a 90° elbow was connected to the south end of this duct. Extensions were connected to this elbow to provide a single exhaust inlet at various heights above the floor. These heights were 3.3 m, 6.3 m, 8.2 m, and 10.2 m (Figure 2).

For the second duct arrangement, sixteen 457 mm diameter ducts were connected to the central duct, as shown in Figure 1. The location of the sixteen exhaust inlets provided by these ducts was scaled to the arrangement with the sixteen inlets used in the small-scale tests. However, for the large-scale tests, the exhaust inlets were located at a single height (10.5 m above the floor).

The north end of the central duct was connected to a vertical duct using two 45° elbows. Two additional 45° elbows were used to connect the lower end of the vertical duct to a horizontal duct at floor level. This duct connected the exhaust system to an axial fan with an approximate rated capacity of 28 $m^3/s$. The fan was located at the exterior of the building. A measuring station including a thermocouple, pitot tube, and gas sampling inlet at the center of the duct was located midway between the last elbow in the duct system and the fan to measure volumetric flow rate and heat release rate. A pitot traverse was conducted to determine the shape factor for the system.

The maximum volumetric flow rate for the exhaust system under ambient conditions was approximately 25 $m^3/s$. This flow rate was used for one series of tests. In addition, tests were conducted with reduced flow rates produced by physically blocking the fan outlet using a perforated steel mesh. Pitot tube traverses were made with and without the blockages to ensure that they did not interfere with the volumetric flow measurements.

The actual volumetric flow rate produced by the fan in a test depended on a number of factors including smoke temperature and the number of exhaust inlets used. Therefore, the volumetric flow rate in the main duct was continuously measured throughout a test. All the measured flow rates were converted to a flow rate at 20°C.

A square propane sand burner was used for the fire source. The burner was capable of simulating fires ranging from 250 kW to 5,000 kW with four possible fire areas: 0.145 $m^2$, 0.58 $m^2$, 2.32 $m^2$, and 9.3 $m^2$. The heat release rate of the fire was determined using two methods. The first method computes the heat release rate from the volume flow rate of propane supplied to the burner. The propane flow rates were measured using rotometers. The second method was based on the oxygen depletion method using the oxygen CO and $CO_2$ concentration, temperature, and volumetric flow rate measured in the main exhaust duct.

With the small heat releases and large volumetric flow rates used for a number of tests, the depletion of oxygen in the exhaust gases was at or below the level for accurate heat release rate measurements using the oxygen depletion method. For these cases, the heat release rate was determined using the measured flow rate of propane into the burner. The oxygen depletion method was used to verify the heat release rate results.

## Instrumentation

The room was instrumented with thermocouples and pitot tubes for velocity measurements. The location of the instrumentation is shown in Figures 1 and 2.

A thermocouple drop was located at the center of the test facility over the propane burner, as shown in Figures 1 and 2. The thermocouples were spaced at 500 mm, starting 1.2 m below the ceiling.

A second thermocouple drop with 19 thermocouples was located at the southeast quarter point of the test facility. These thermocouples were spaced at 500 mm with the highest thermocouple located at the ceiling. The data obtained using these thermocouples were used to determine the height of the smoke layer.

In the multi-inlet tests, a set of 16 thermocouples was located below the southeast duct inlet (Location 3a in Figures 1 and 2). The thermocouples were centered on the exhaust duct with the top thermocouple located at the inlet 10.5 m above the floor. These thermocouples were used to measure the temperature below the exhaust inlet.

In the tests with a single exhaust inlet, a thermocouple drop with 16 thermocouples was located on the centerline of the duct (Location 3b in Figures 1 and 2). The thermocouples were spaced at 0.5 m. In the case with the duct inlet at a height of 3.3 m, the lowest thermocouple was at 2.3 m above the floor. For the other three test configurations, the lowest thermocouple was 0.9 m above the floor. For the configuration with the duct inlet 6.3 m above the floor, five thermocouples were located on the centreline of the duct with the highest thermocouple approximately 2 m above the inlet. With the duct inlet at a height of 8.2 m and 10.2, the highest thermocouple was at the same height as the duct inlet and 2 m below the duct inlet, respectively.

The volume flow rate, temperature, CO, $CO_2$, and oxygen concentrations were measured in the main exhaust duct. These measurements were used to determine the heat release rate of the fire, as well as to calculate the exhaust rate of the ventilation system. A pitot tube and thermocouple located at the center of the duct system were used to determine the volumetric flow rate in the duct.

## Test Procedure

Most tests conducted in the facility described in the previous section were conducted over an extended period of time (up to one hour). The test procedure was as follows:

1. All systems, including the mechanical exhaust system and data acquisition system, were started.
2. A small burner was ignited and the propane flow rate was adjusted to provide a low heat release rate fire.
3. All conditions in the test facility were monitored continuously using the data acquisition system.
4. The conditions in the test facility were allowed to stabilize for approximately 15 minutes, producing a steady clear height with upper-layer exhaust.
5. The heat release rate was increased and Steps 3 and 4 repeated.

Using this test procedure, data could be acquired for several heat release rates under the same test conditions.

## Test Parameters

The main parameters that were varied in the tests conducted using the large-scale facility were as follows:

1. *Heat release rate.* Tests were conducted with the following nominal heat release rates: 250 kW, 500 kW, 600 kW, 1000 kW, 1500 kW, 2000 kW, 2500 kW, 3000 kW, 4000 kW, and 5000 kW.
2. *Number of exhaust inlets.* Tests were conducted with one and sixteen exhaust inlets. The single exhaust inlet was 1.2 m in diameter. The 16 exhaust inlets were 457 mm in diameter. The locations of the exhaust inlets are shown in Figures 1 and 2.
3. *The exhaust inlet height.* A single height, 10.5 m, above the floor was used for the tests with 16 exhaust inlets. For a single exhaust inlet, tests were conducted with the exhaust inlet 3.3 m, 6.3 m, 8.2 m, and 10.2 m above the floor.
4. *Volumetric flow rate.* Tests were conducted with three nominal volumetric flow rates. The maximum volumetric flow rate at 20°C was approximately 25 $m^3/s$. This flow rate was used for one series of tests. In addition, partial blocking of the main duct was used to produce a medium and low flow rate. The volumetric flow rate produced by the exhaust system depends on several factors. The actual flow rate at the time other measurements in the facility were taken is determined using the data obtained from the measuring station located in the main duct.

## Scaling

For the range of heat release rates used in the test facility (250 kW to 5 000 kW) and using Equation 7, the physical model tests provide physical scalings ranging from approximately 1/1 to 1/3 for a 5,000 kW steady-state design fire. The tests thus simulate atria with heights ranging from approximately 12.2 m to 36.6 m.

For a 2,000 kW design fire, the tests provide physical scaling in the range of approximately 1/1 to 1/2.25, simulating atria with heights ranging from approximately 12.2 m to 28 m.

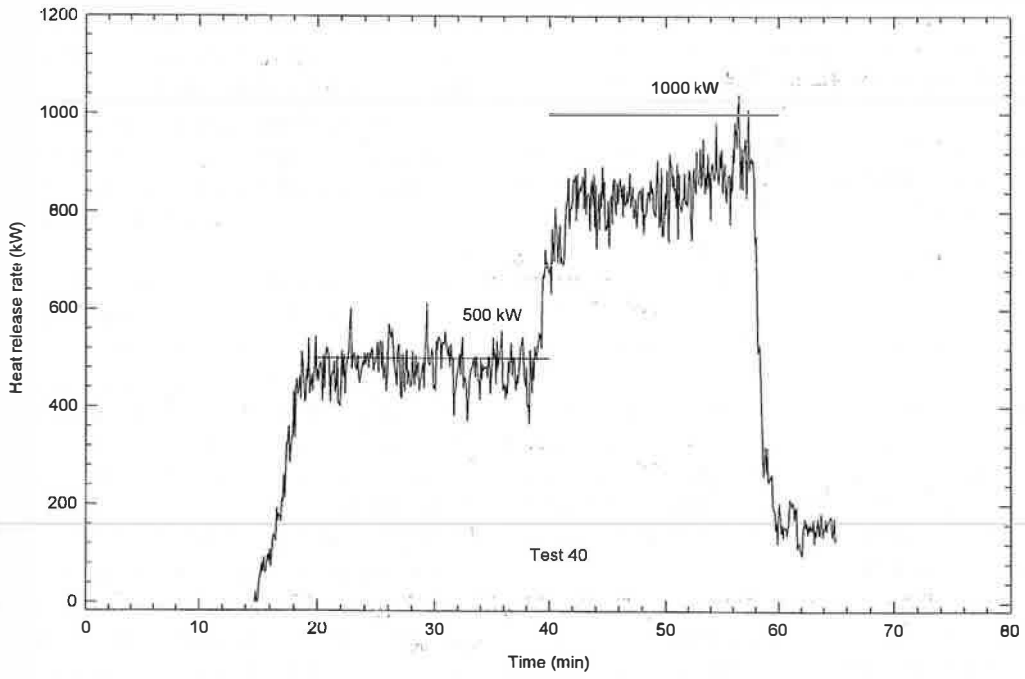


***Figure 3*** *Heat release rate for large-scale test.*

## Steady-State Test Conditions

As discussed in the test procedure, the propane flow rate was adjusted to a predetermined level to produce the required heat release rate. Figure 3 shows the heat release rates measured using the oxygen depletion method. Also shown are the nominal heat release rates for the tests.

The original estimates of the propane flow rates to produce the nominal heat release rate were based on literature values for propane density. Because of fillers in the commercial propane used for the tests, the actual density of the propane was lower than the literature value. This variation in the propane density produced an approximately 10% decrease in the heat release rates for the tests compared with the nominal values. The resulting heat release rates for each test are summarized in Table 1.

The fire was steadily maintained for 10 to 20 minutes at each heat release rate to allow stable conditions to be reached in the test facility.

The temperature profiles measured at various heights in the test facility are given in Figure 4 for the heat release rates shown in Figure 3. The radiation from the fire produces some heating of the walls and air in the lower levels of the test facility, especially for high heat release rate fires. As a result, the temperature profiles in the upper layer did not reach a steady condition. However, in the later stages of the test with a given heat release rate, the temperature increase was minimal.

## Steady-State Temperature Profiles

Subsequent to the tests, the time-temperature data were analyzed to determine the temperatures at the various locations in the test facility at the end of the steady-state phase. These temperatures were used to determine the steady-state temperature profiles at the quarter-point of the room (Location 2 in Figure 2) and at the duct inlet (Location 3a for tests with 16 duct inlets and Location 3b for tests with a single duct inlet). Temperature profiles for all tests are provided in the final report for the project (Hadjisophocleous et al. 1998).

Figures 5 and 6 show the temperature profile measured for tests with the nominal 1500 kW heat release rate and 16 exhaust inlets located 10.5 m above the floor. The results are typical of cases in which there was a well-developed smoke layer below the exhaust inlets (heat release rate of 1000 kW or higher).

Because of the variation in the ambient temperature from test to test, the initial temperature was subtracted from the measured temperature. As such, the temperature profiles show the temperature difference produced by the fire rather than the actual temperatures measured in the specific test.

With the extended time period used to obtain steady conditions, there was some heating of the air below the smoke layer. For the tests shown in Figures 5 and 6, the temperature in the lower layer was increased by 10°C. This increase in the lower temperature ranged from approximately 1°C for the nominal 250 kW tests to 40°C for the tests at 5000 kW.

## Upper and Lower Layer Temperature

As shown in Figure 5, the temperature profiles for the steady-state portion of the tests typically had temperature plateaus in the hot and cold layers. The temperatures in these two areas were averaged to determine the upper ($T_u$) and lower

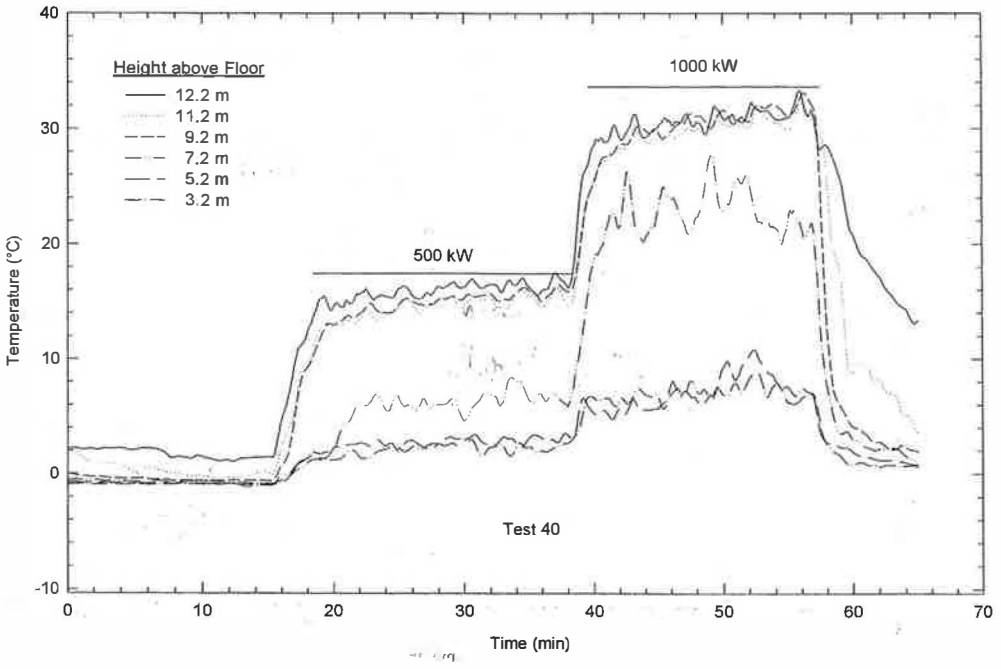


***Figure 4*** *Temperatures at room quarter point.*

**TABLE 1 (Continued)**
**Results for Large-Scale Tests**

| Test Num. | Heat Release Rate (kW) | Num.of Inlets | Inlet Height (m) | Vol. Flow Rate ($m^3/s$) | Smoke Prod. ($m^3/s$) | Smoke Height ($\Delta T_{80}$) (m) | Smoke Depth ($\Delta T_{80}$) (m) | Smoke Height ($\Delta T_{20}$) (m) | Smoke Depth ($\Delta T_{20}$) (m) | Trans. Zone Depth (m) | $\Delta T$ Upper Layer (°C) | $\Delta T$ Duct (°C) | Adiab. $\Delta T$ (°C) | $CO_2$ Duct (%) |
|---|---|---|---|---|---|---|---|---|---|---|---|---|---|---|
| L-30 | 3600 | 1 | 6.3 | 15.2 | 15.9 | 5.1 | 1.2 | 4.7 | 1.5 | 0.4 | 111.2 | 95.4 | 131 | 0.56 |
| L-31 | 3600 | 1 | 6.3 | 19.5 | 15.9 | 5.1 | 1.2 | 4.8 | 1.4 | 0.3 | 96.7 | 79.6 | 131 | 0.47 |
| L-36 | 3600 | 1 | 8.2 | 20.1 | 19.3 | 5.9 | 2.3 | 5.3 | 2.9 | 0.6 | 91.8 | 85.6 | 108 | 0.53 |
| L-39 | 3600 | 1 | 8.2 | 14.5 | 17.2 | 5.4 | 2.8 | 4.6 | 3.6 | 0.8 | 107.2 | 99.9 | 122 | 0.34 |
| L-42 | 3600 | 1 | 10.2 | 13.7 | 17.6 | 5.5 | 4.7 | 4.8 | 5.4 | 0.7 | 105.2 | 97.2 | 119 | 0.62 |
| L-45 | 3600 | 1 | 10.2 | 18.5 | 18.4 | 5.7 | 4.5 | 4.9 | 5.3 | 0.8 | 99.0 | 92.6 | 113 | 0.57 |
| L-2 | 4500 | 16 | 10.5 | 19.9 | 22.8 | 6.2 | 4.3 | 5.3 | 5.2 | 0.8 | 91.5 | 88.4 | 114 | |
| L-11 | 4500 | 16 | 10.5 | 19.7 | 23.4 | 6.3 | 4.2 | 5.4 | 5.1 | 0.9 | 93.3 | 92.2 | 111 | 0.57 |
| L-12 | 4500 | 16 | 10.5 | 17.8 | 24.8 | 6.6 | 3.9 | 5.5 | 5.0 | 1.1 | 127.3 | 131.1 | 105 | 0.84 |
| L-27 | 4500 | 1 | 3.3 | 16.8 | 14.2 | 4.1 | -0.8 | 3.4 | -0.1 | 0.7 | 145.8 | 43.6 | 184 | 0.27 |
| L-29 | 4500 | 1 | 6.3 | 14.1 | 18.2 | 5.2 | 1.1 | 4.8 | 1.5 | 0.4 | 129.8 | 117.1 | 143 | 0.75 |
| L-33 | 4500 | 1 | 6.3 | 20.5 | 32.5 | 8.0 | -1.7 | 5.0 | 1.3 | 3.0 | 116.7 | 103.8 | 80 | 0.64 |
| L-36 | 4500 | 1 | 8.2 | 18.3 | 19.6 | 5.5 | 2.7 | 4.8 | 3.4 | 0.7 | 120.2 | 111.8 | 133 | 0.67 |
| L-39 | 4500 | 1 | 8.2 | 14.0 | 18.2 | 5.2 | 3.0 | 4.3 | 3.9 | 0.9 | 137.3 | 128.0 | 143 | 0.81 |
| L-42 | 4500 | 1 | 10.2 | 13.3 | 18.7 | 5.3 | 4.9 | 4.3 | 5.9 | 1.1 | 136.8 | 126.7 | 140 | 0.78 |
| L-45 | 4500 | 1 | 10.2 | 17.0 | 20.1 | 5.6 | 4.6 | 4.6 | 4.6 | 1.1 | 127.6 | 119.5 | 130 | 0.75 |

($T_l$) layer temperatures for use in determining the smoke interface height.

The average temperature for the upper layer for each test is given in Table 1. As discussed previously, the initial ambient temperature was subtracted from the temperature data, and the upper-layer temperatures provided in the table are an estimate of the temperature difference produced by the fire.

## Smoke Interface

The steady-state temperature profiles measured at Location 2 (Figure 1) were used to determine information regarding the height of the smoke interface, the thickness of the smoke transition zone, and the temperature in the upper layer. The method for estimating the smoke interface heights based on a limited number of temperature measurements over the height of the facility was described previously. For the large-scale tests, Equation 9 was used to provide estimates for the height of the bottom and top of the transition zone as follows:

1. *Smoke height* ($H_{T20}$). This height was determined by interpolating the temperature data to determine the height at which the temperature difference between the hot and cold layers was 0.2 ($T_u - T_l$). This gives a smoke interface height near the bottom of the transition zone. ($T_u$ and $T_l$ are the average temperatures in the upper and lower layer, respectively.)
2. *Smoke height* ($H_{T80}$). This height was determined by interpolating the temperature data to determine the height at which the temperature difference between the hot and cold layers was 0.8 ($T_u - T_l$). This gives a smoke interface height near the top of the transition zone.

Based on the two smoke interface heights, two estimates for the depth of the smoke layer below the exhaust inlets can be determined. These are $SD_{T80}$ and $SD_{T20}$, which give the depth of the smoke layer based on the smoke interface height estimates $H_{T80}$ and $H_{T20}$, respectively. In addition, an estimate of the thickness or depth of the transition zone $TD_T$ is provided ($H_{T80} - H_{T20}$).

The smoke interface heights estimated for all large-scale tests are summarized in Table 1.

## Measurements in the Duct

Several parameters were measured in the main exhaust duct including temperature and $CO_2$ concentrations. The results for these measurements are given in Table 1. In addition, the measurements made in the duct were used to determine the volumetric flow rate in the duct. These results were converted to the equivalent volumetric flow rate at 20°C.

## Smoke Production and Adiabatic Temperature

For an upper layer with little heat transfer to the atrium walls and ceiling and small radiative heat transfer from the

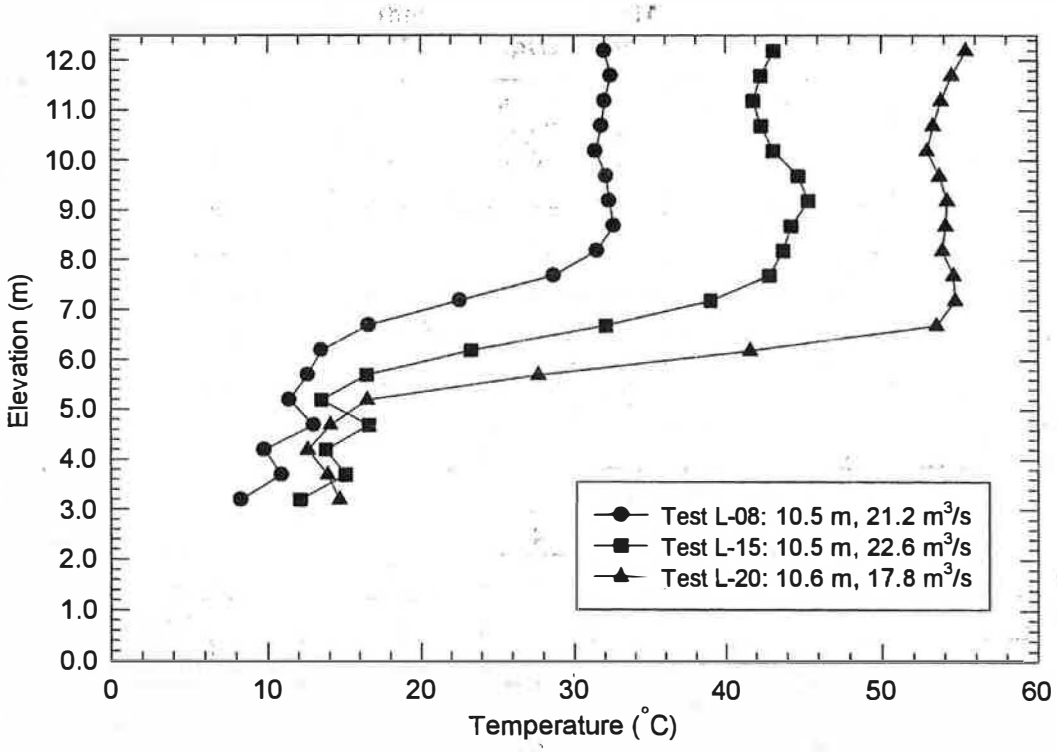


***Figure 5*** *Quarter-point temperature profiles for 1500 kW tests and 16 ports.*

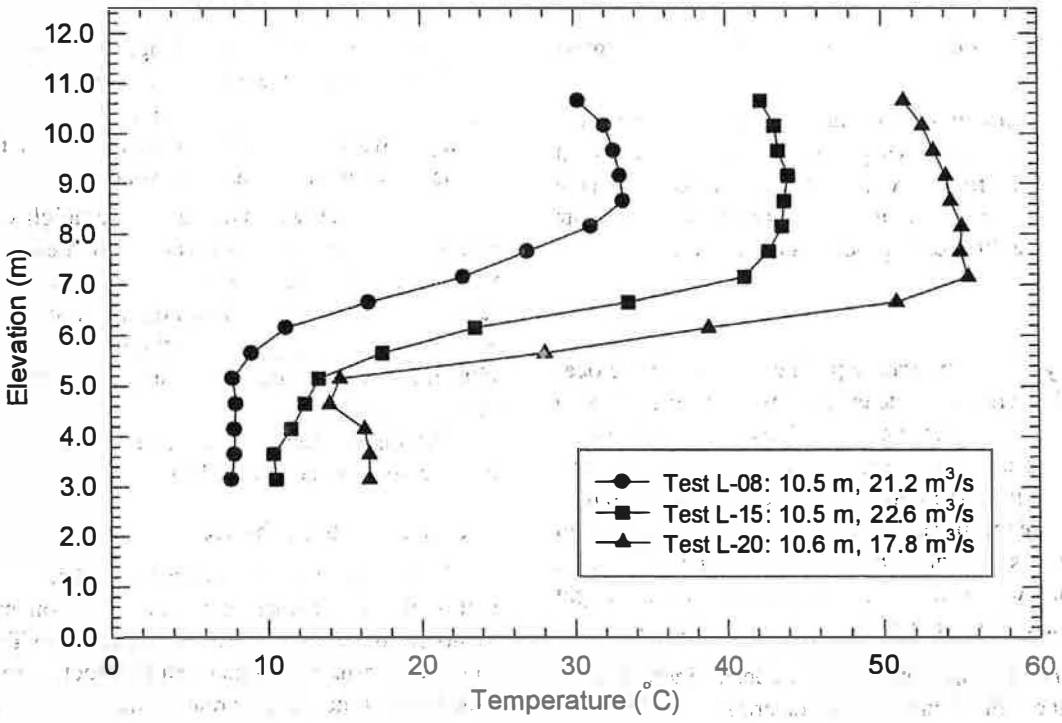


***Figure 6*** *Temperature profiles below duct inlet for 1500 kW tests and 16 ports.*

smoke layer, the upper layer can be thought of as adiabatic or as having negligible heat transfer (Klote 1994). Under such conditions, Equation 2 can be used to estimate the average temperature in the upper layer and the temperature in the exhaust gases.

Design guides such as NFPA 92B (NFPA 1995) provide equations for estimating the mass flow rate of smoke into the hot upper layer (Equation 1). Using the upper layer height determined experimentally ($H_{T80}$), this equation was used to estimate the mass flow rate into the upper layer. In order to provide a comparison with measured exhaust rate, this flow rate was converted to a volumetric flow rate of smoke into the upper layer using Equation 2 for the adiabatic plume temperature and the ideal gas law (Equation 3). The results were converted to an equivalent flow rate at 20°C. The calculated smoke production rates and adiabatic temperatures are given in Table 1.

The calculations for smoke flow rate into the upper layer and upper layer temperature were carried out using the simple plume method included in the ASMET set of engineering tools (Klote 1994). For these calculations, the convective heat release rate was assumed to be 70% of the measured total heat release rate. A comparison of the increase in upper layer temperature measured experimentally with the model results is shown in Figure 7. The results indicate that the adiabatic temperature increase tends to be slightly higher than the experimental result. However, considering the wide range of test parameters, there is a good correlation between the measured and estimated temperature increase.

A correlation between the measured upper-layer temperature and the temperature measured in the duct is shown in Figure 8. The temperatures measured in the duct were lower than those measured in the compartment.

There was a substantial length of duct (> 30 m) between the compartment and the measuring station in which heat could be lost through the duct wall. However, the difference in duct and upper layer temperature was not proportional to temperature. This indicates that heat transfer losses from the exhaust duct were not the only factor producing the temperature difference.

The test conditions under which there were major differences in the two temperatures were those in which the smoke layer was near to or above the duct inlet, resulting in cold air being entrained into the exhaust.

## Smoke Exhaust Rate—Large-Scale Tests

Equation 1 can be used to calculate the mass flow rate of smoke into the upper layer. For a steady process, it also defines the amount of smoke exhausted using the fan system. In an ideal smoke management system, the smoke exhaust rate should be equivalent to the rate of smoke production. However, in the physical model tests, one objective was to investigate situations in which the smoke exhaust system was not operating at maximum efficiency. This was accomplished by locating the exhaust inlets at levels near or below the level at which the steady-state smoke interface would normally occur for a specified condition (volumetric exhaust rate and heat release rate). Under these conditions, cold air was entrained with the smoke produced by the fire.

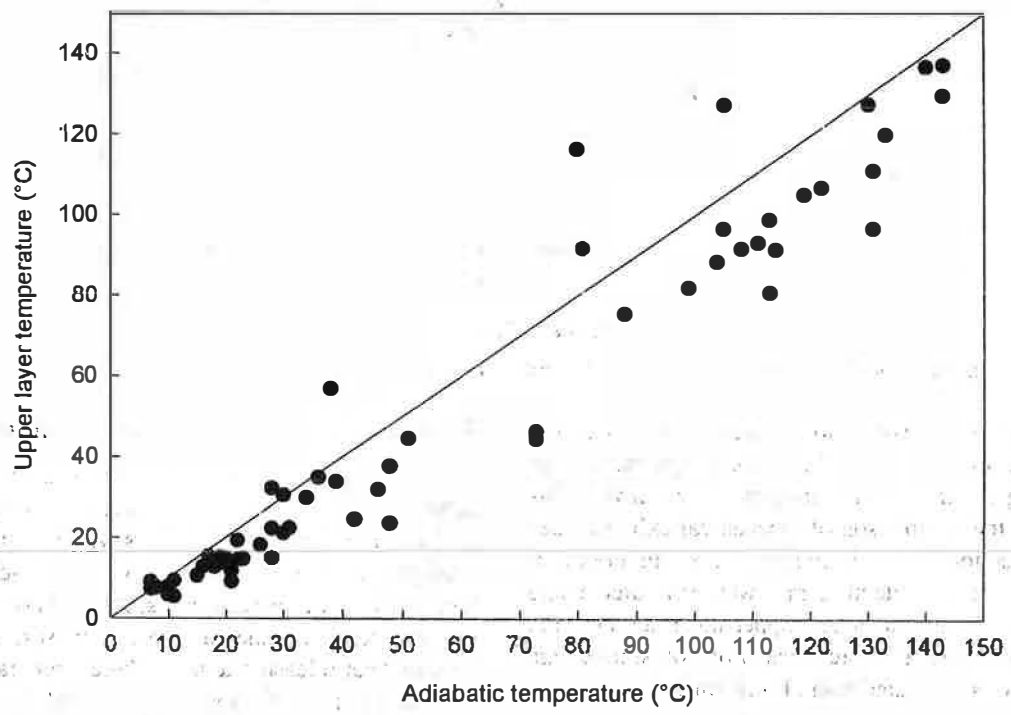


***Figure 7*** *Correlation of adiabatic and upper layer temperature for large-scale tests.*

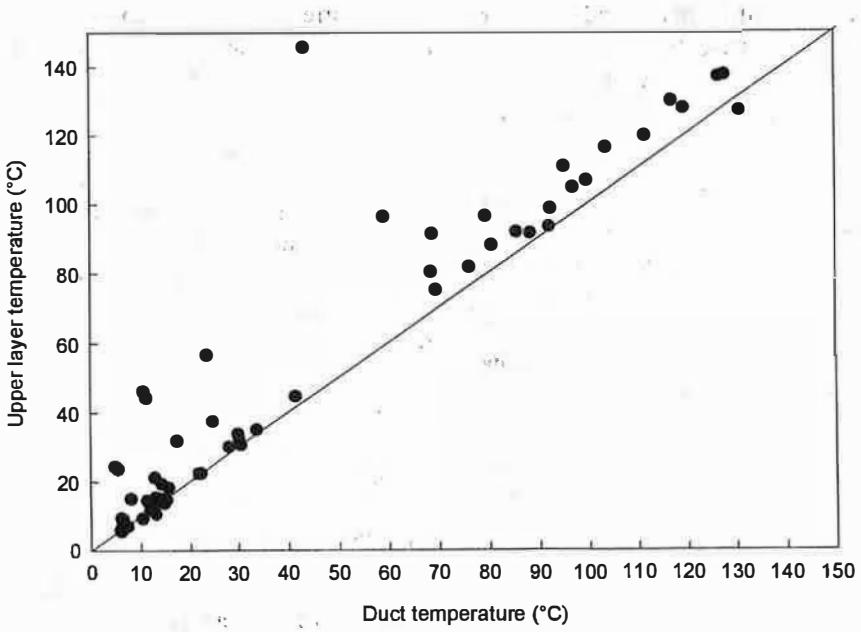


***Figure 8*** *Correlation of duct and upper layer temperature for large-scale tests.*

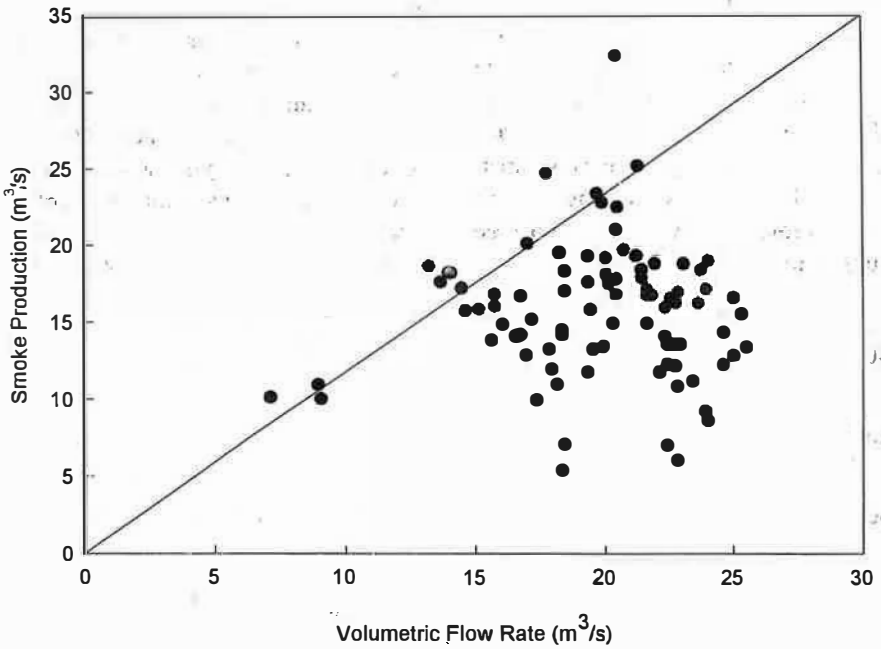


***Figure 9*** *Correlation of smoke production with exhaust rate for large-scale physical model.*

In practice, it was possible to produce situations with a high percentage of the air in the exhaust system (up to 75%) consisting of air entrained from the lower layer. This is illustrated by the comparison of mechanical exhaust rates vs. smoke production shown in Figure 9. For this comparison, the smoke mass production rate was estimated using Equation 1. Using the calculated upper-layer temperature and the ideal gas law, the volumetric flow of smoke into the upper layer was estimated using Equation 3.

## Results for Tests with 16 Exhaust Inlets

The results for the tests with 16 exhaust inlets located 1.7 m below the ceiling can be grouped into two categories based on the heat release rate. For tests with measured heat release rates greater than 900 kW, there was a well-developed smoke layer below the inlets and the estimated smoke production rate was comparable to the measured exhaust rate (Figure 9). For the low heat release rate tests, there were cases in which the measured volumetric flow rate exceeded the estimated smoke production by up to a factor of 2. The results for each group of tests are discussed in the following sections.

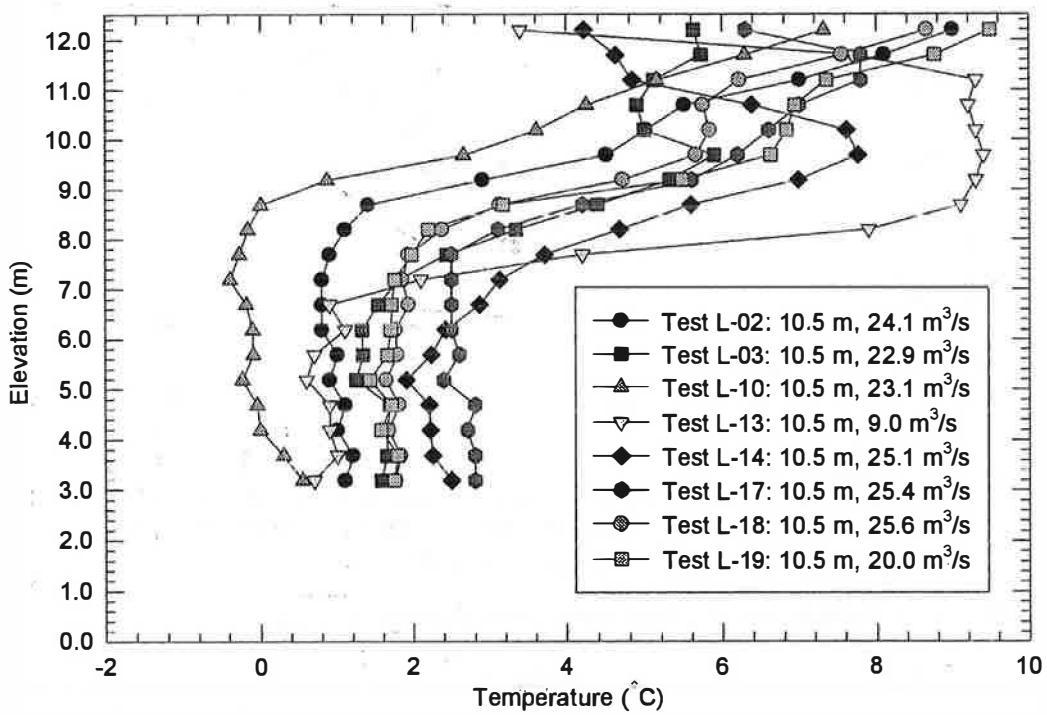


***Figure 10*** *Quarter-point temperature profiles for 225 kW tests and 16 ports.*

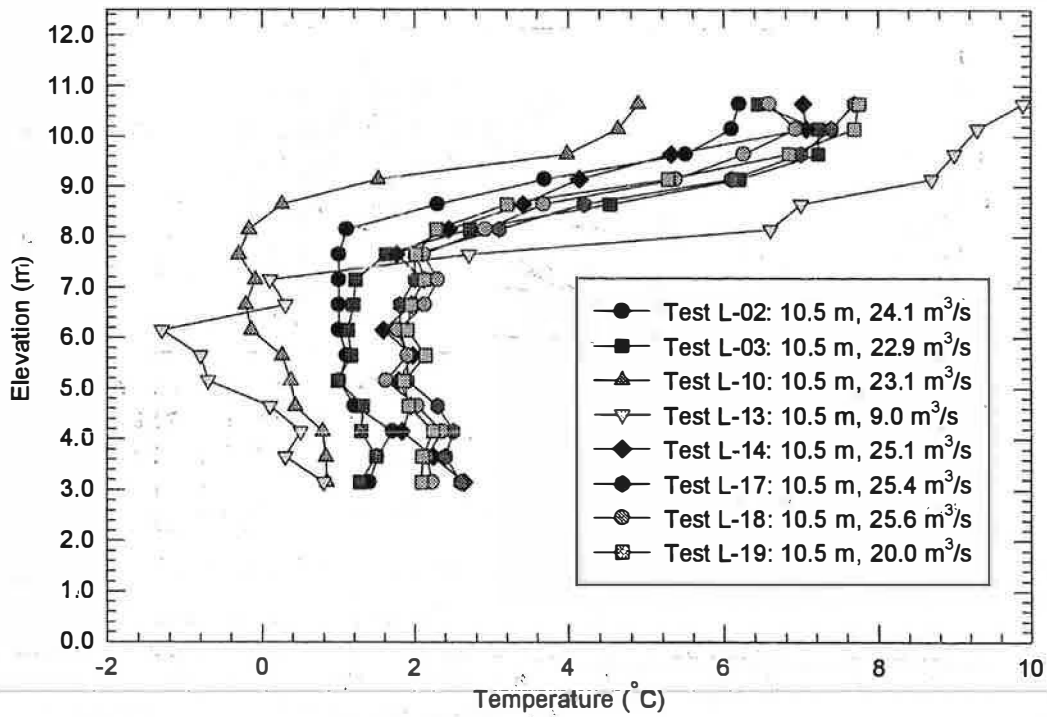


***Figure 11*** *Temperature profiles below duct inlet for 225 kW tests and 16 ports.*

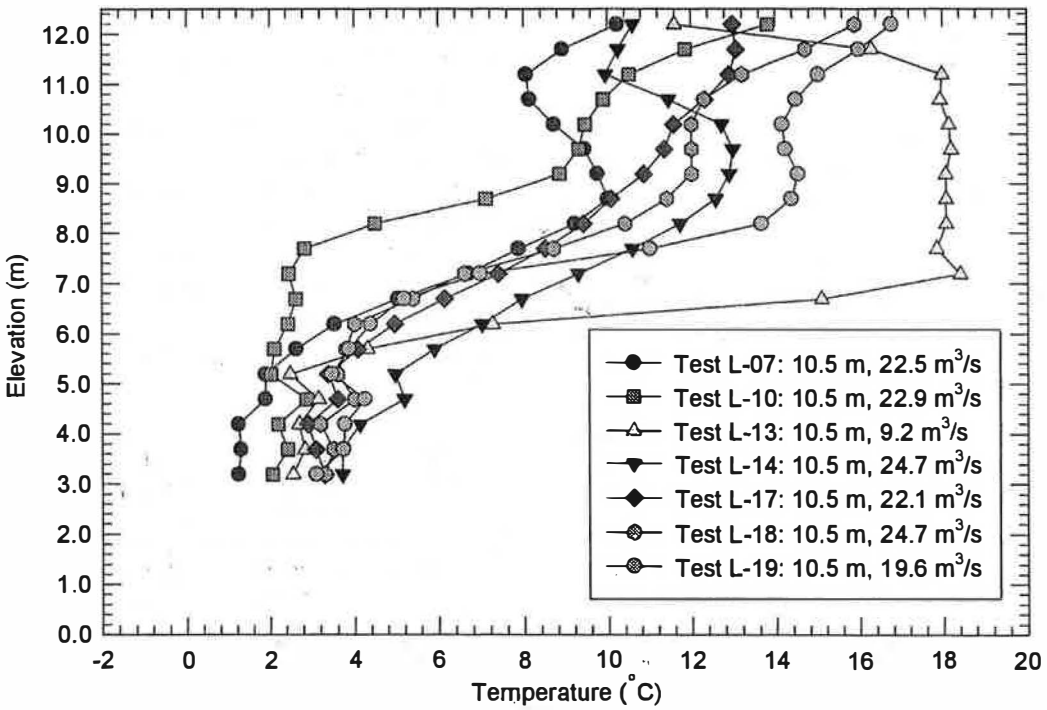


***Figure 12*** *Quarter-point temperature profiles for 450 kW tests and 16 ports.*

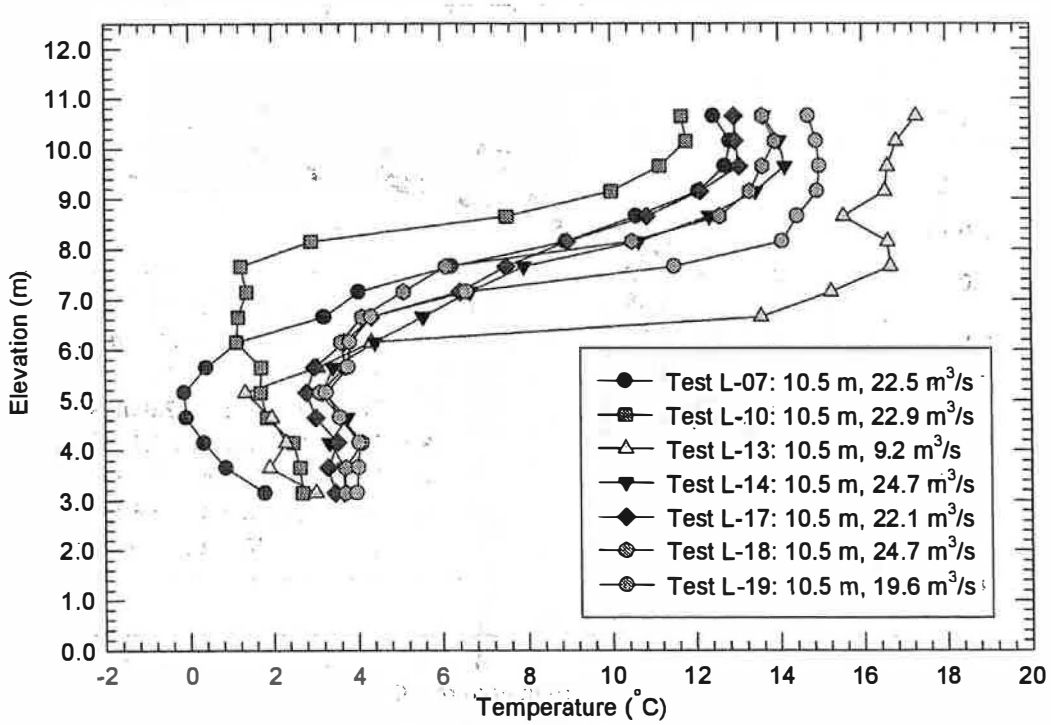


***Figure 13*** *Temperature profiles below duct inlet for 450 kW tests and 16 ports.*

however, a small decrease in the temperature at the height of the exhaust inlet relative to the temperatures above and below this height. This would suggest that there might be some mixing of the air from the cold lower layer into the upper layer due to the exhaust system.

The temperature profiles measured below the duct inlet and at the facility quarter-point are comparable (Figure 16). Also, the temperature measured at the center of the duct inlet is comparable to the temperature measured at the same elevation in the test facility and the temperature measured in the main exhaust system.

The upper layer and duct temperatures measured in the high heat release tests with 16 exhaust inlets (Table 1) are comparable. With a well-developed smoke layer formed below the duct inlet, the air in the exhaust system is predominantly from the upper hot layer.

The temperature profiles became more stable as the smoke depth below the duct inlet increased. Consistent results were obtained when the upper or 80% temperature difference interface was 1 m to 2 m below the duct inlet.

The smoke interface heights ($H_{T80}$ and $H_{T20}$), as well as the depth of the transition zone and the duct inlet height, are shown in Figure 17 for tests with heat release rates of 2700 kW. Tests 1 through 8 were conducted with the 16 duct inlets and the remaining tests with the single exhaust inlet. The latter tests will be discussed in the next section.

The interface heights are dependent on the exhaust rate with the $H_{T80}$ interface at a height of 6 m to 7 m and the $H_{T20}$ interface at a height of 5 m to 6 m. The transition depth was approximately 0.8 m to 1.0 m.

## Tests with a Single Exhaust Inlet

A series of tests were conducted with a single large exhaust inlet at various heights (3.3 m, 6.3 m, 8.2 m, and 10.2 m above the floor). The temperature profiles at the room quarter-point and at the duct inlet are given in the final report for the project (Hadjisophocleous et al. 1998). With the duct inlet at 8.2 m and 10.2 m, duct thermocouples were all located below the inlet height. For the tests with the inlet at 3.3 m and 6.3 m, several thermocouples were located inside the duct on the centreline.

The temperature profiles for a series of tests at 3600 kW are shown in Figures 18 and 19. For these tests, the temperature profiles at the room quarter-point are similar to those obtained with the 16 duct inlets. That is, there are four distinct temperature zones, as follows:

1. A hot upper layer in which the temperature does not vary substantially with height.
2. The hottest region, located immediately above the transition zone. Since the room quarter-point was only 6 m from the fire, there could be some direct heating into the lower smoke interface. Also, the CFD modeling results indicate there was some mixing of the cold air from the lower layer into the upper layer (Hadjisophocleous et al. 1999).
3. A transition zone between 5 m and 6 m with a rapid change in temperature.
4. A cold lower layer in which the temperature does not vary substantially with height. Due to extended heating from the fire, this zone was approximately 20°C above ambient temperature.

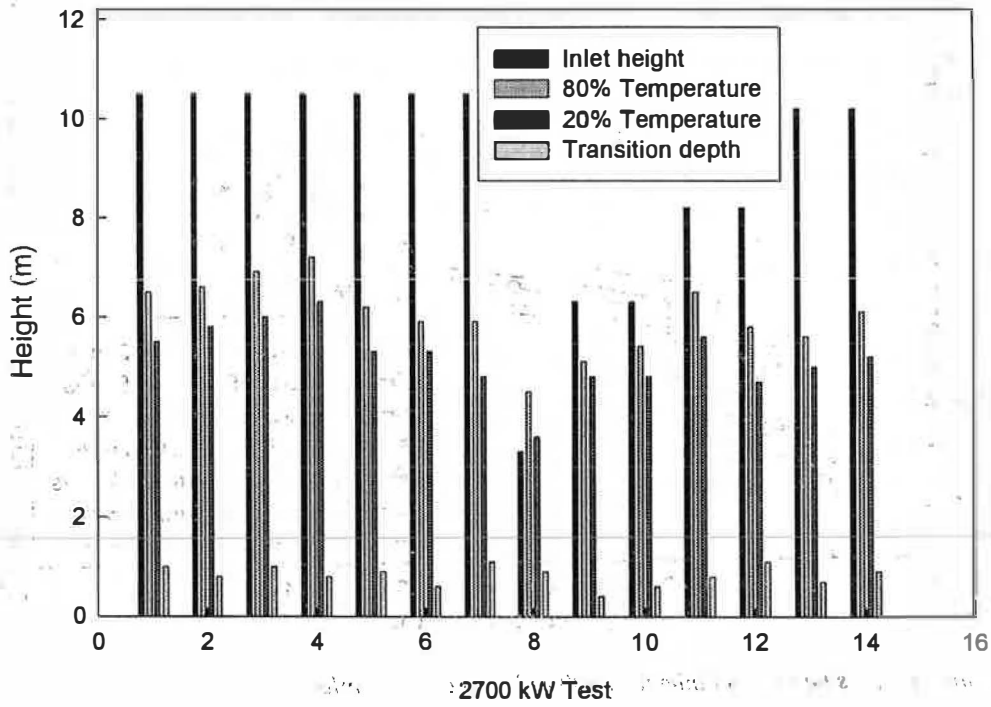


***Figure 17*** *Steady-state smoke layer results for 2700 kW heat release rate tests.*

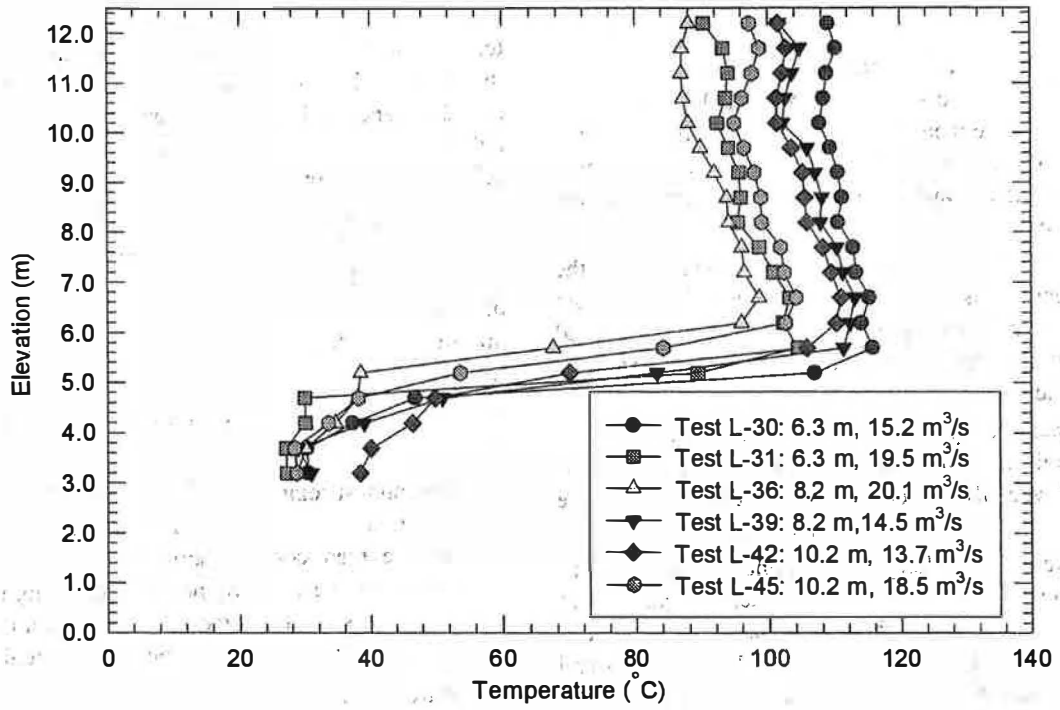


***Figure 18*** *Quarter-point temperature profiles for 3600 kW tests and one inlet.*

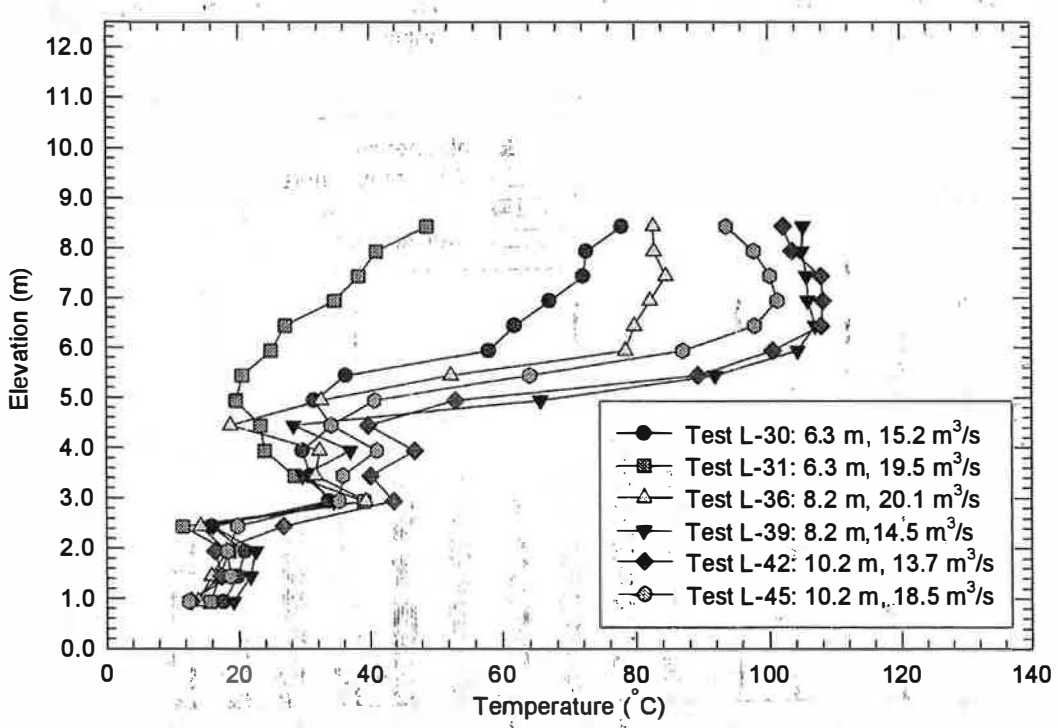


***Figure 19*** *Temperature profiles below duct inlet for 3600 kW tests and one inlet.*

The temperature profiles measured at the duct inlet varied. For tests L-39, L-42, and L-45, the temperature profiles below the duct were comparable to those measured at the room quarter-point. For these cases, the smoke layer below the inlet was well developed and the air entrained in the exhaust inlet was primarily from the hot layer. The upper layer and duct temperatures are also comparable (Table 1).

For Test L-36, the temperatures measured below the duct inlet were slightly lower than those measured at the same height at the room quarter-point. This would indicate that some air was being entrained from the lower layer in this case.

For Tests L-30 and L-31, with the duct inlet at 6.3 m, the temperatures measured below and inside the duct on the centerline were substantially cooler than those measured at the same height at the room quarter-point. In these tests, air was being drawn from the lower layer up into the duct. However, the temperature on the centerline of the duct above the height of the inlet increased as the air in the exhaust inlet was mixed. This suggests that much of the flow into the duct was from the surrounding hot layer. This is consistent with the duct temperature results, which showed a 20% temperature decrease compared to the upper-layer temperature.

The smoke interface heights, as well as the duct inlet height and the transition depth, are shown in Figure 20 for the 3600 kW tests. These results indicate that the smoke interface heights are relatively constant from test to test. The 20% temperature increase height was relatively constant for the tests, taking into consideration the differences in exhaust rates from test to test. The 80% temperature interface was lower with the duct inlet at the 6.3 m height. This indicates there was a decrease in exhaust efficiency in this case.

The smoke interface height results were similar in the tests at 2700 kW, as shown in Figure 17. Also shown in this figure are the results for tests with 16 duct inlets. The smoke interface heights measured with the single exhaust inlet are comparable to, but generally lower than, those obtained with the 16 exhaust inlets. This suggests that the exhaust system with a single exhaust inlet is generally less efficient than the system with 16 exhaust inlets.

The duct and upper-layer temperatures given in Table 1 also indicate the decreased efficiency. For tests with the single exhaust inlet, there is an increased temperature difference, indicating more mixing of air from the cold layer into the exhaust system.

The interface heights for the tests with the single exhaust inlet at 6.3 m are shown in Figure 21. The heat release rates for the tests were as follows: Tests 1 and 2, 450 kW; Tests 3 and 4, 900 kW; Tests 5 and 6, 1800 kW; Tests 7 and 8, 2700 kW; Tests 8 and 9, 3600 kW; and Tests 11 and 12, 4500 kW.

For the low heat release rate tests, the interface height is near the inlet height. For higher heat release rates, a smoke layer developed below the exhaust inlet reaching a depth of 1 m to 1.5 m. In all cases, the parameters indicate there was some cold air entrainment into the exhaust system. Also, there are indications that the exhaust system was extracting smoke from above the inlet height. This is demonstrated in the results for Test 12 shown in Figure 21 (Test L-27) in which the $H_{T80}$ interface was well above the inlet height. The heat release rate for this test was 4500.

Figure 22 shows the interface heights for a series of tests with the single duct inlet at 8.2 m. For these tests, the clear height is dependent on the heat release rate and volumetric

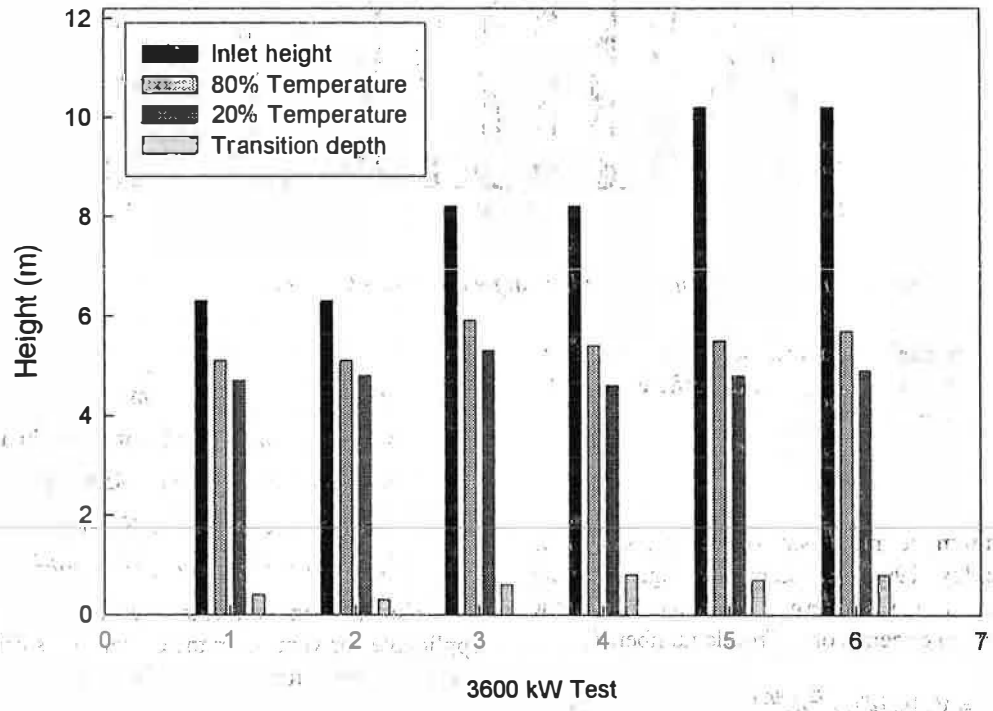


***Figure 20*** *Steady-state smoke layer results for 3600 kW heat release rate tests.*

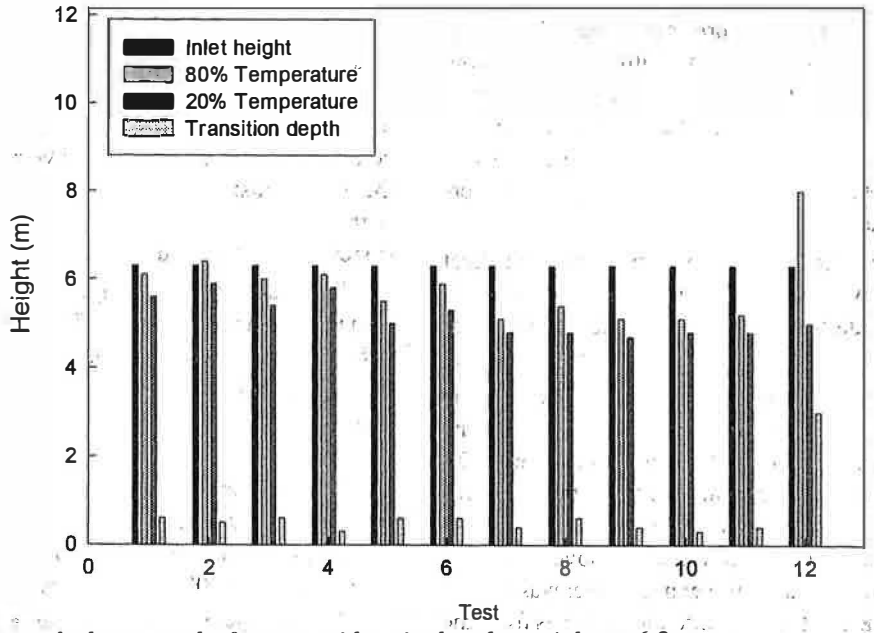


***Figure 21*** *Steady-state smoke layer results for tests with a single exhaust inlet at 6.3 m.*

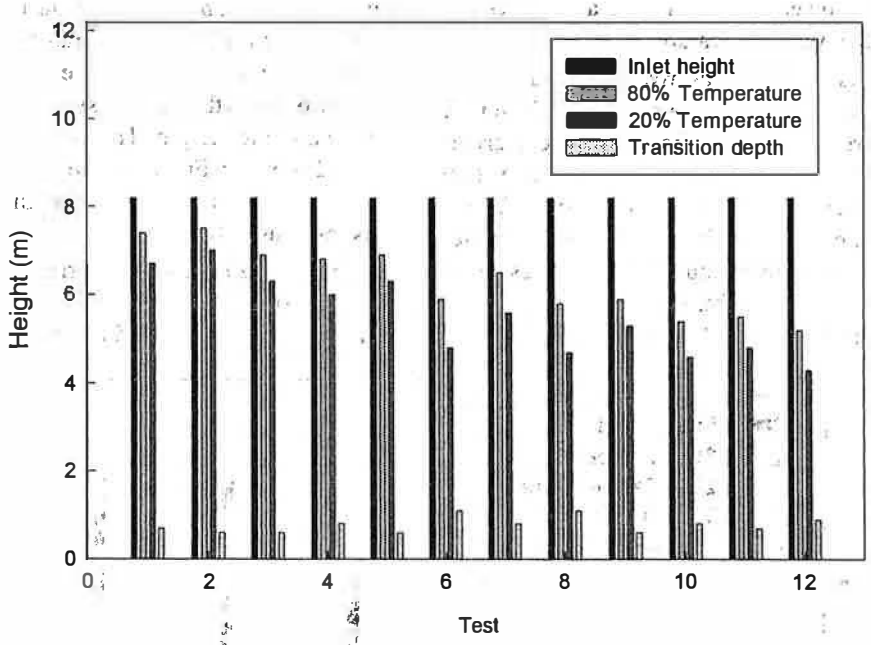


***Figure 22*** *Steady-state smoke layer results for tests with a single exhaust inlet at 8.2 m.*

flow rates. Also, for the higher heat release rates for which the smoke depth below the inlet was > 2 m, the efficiency of the exhaust system was improved.

## PLUGHOLING

Cold air entrainment into a smoke venting system is addressed by Hinckley (1995). Based on investigations with gravity venting systems, it was determined that the onset of the plugholing phenomena depends on a Froude number, $F_c$:

$$F_c = V_v/[(g\theta/T_o)^{1/2} d_e^{5/2}] \quad (10)$$

where

$V_v$ = volume rate of flow, $m^3/s$;

$d_e$ = depth of hot gases below the exhaust inlet, m;

$\theta$ = temperature above ambient, K;

$T_o$ = ambient temperature, K; and

$g$ = acceleration due to gravity, $m/s^2$.

Work on vents indicates that a Froude number of 1.5 is applicable for vents near the center of a smoke reservoir and 1.1 is applicable for vents near the sides (Morgan and Gardiner 1990).

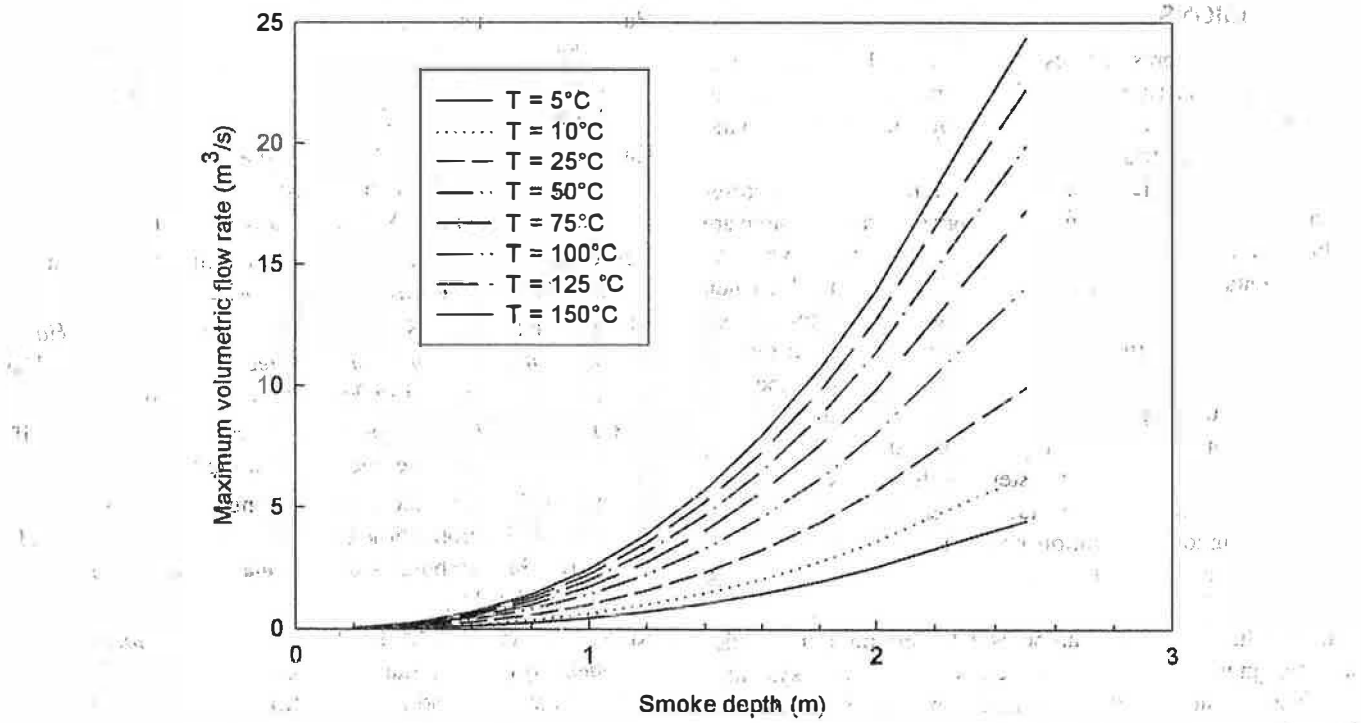


***Figure 23** Maximum volumetric flow vs. smoke depth.*

Hinckley (1995) defines Equation 10 in terms of the smoke depth. However, the equation was developed assuming the smoke vent systems were located at the ceiling. In the following analysis, it is assumed that the smoke depth in Equation 10 represents the distance between the exhaust inlet and the clear height.

Plots for maximum volumetric flow rate vs. smoke depth are shown in Figure 23 for smoke temperatures of 5°C, 10°C, 25°C, 50°C, 75°C, 100°C, 125°C, and 150°C above ambient using a Froude number of 1.1. The temperature increases are representative of those measured in the physical model tests.

For the small-scale physical model tests, the volumetric flow rate per exhaust inlet was in the range of 0.1 $m^3/s$ to 0.5 $m^3/s$, depending on the number of exhaust inlets that were open and the operating speed of the fan. For this volumetric flow range, Figure 23 indicates that air entrainment would occur for smoke depths between 0.5 m and 1.0 m for the range of temperatures produced in the test program. The results of the small-scale physical model tests were consistent with the analysis based on Equation 10 (Lougheed and Hadjisophocleous 1997).

For the large-scale tests with the 16 exhaust inlets, the volumetric flow rate per inlet ranged from 0.5 $m^3/s$ to 1.5 $m^3/s$. Based on Figure 23, air entrainment would become a problem for smoke depth in the range of 0.5 m to 1.5 m, depending on the temperature in the upper zone. Also, the probability of entraining air from the lower layer increases as the temperature in the upper layer decreases. Overall, the large-scale tests are consistent with this analysis. Typically, the exhaust system is efficient if the smoke layer depth below the height of the exhaust inlet meets the requirements shown in Figure 23.

For the large-scale physical model tests with a single exhaust inlet, the volumetric flow rates ranged from 10 $m^3/s$ to 25 $m^3/s$. The analysis shown in Figure 23 indicates the smoke depth below the exhaust inlet should be 1.5 m to 3.0 m for an efficient exhaust system. This is consistent with the large-scale results.

The small- and large-scale physical model tests covered a broad range of volumetric flow rates through exhaust inlets (0.25 $m^3/s$ to 25 $m^3/s$). The results indicate that Equation 10 can be used to estimate the conditions for which an efficient smoke exhaust system can be designed.

Relatively thin smoke layers (< 0.25 m) were measured below the exhaust inlet in some situations. However, in these cases, the exhaust rate was much greater than the smoke production rate (> 2.1) indicating air entrainment from the cold layer along with the smoke produced by the fire. However, as the heat release rate and thus the rate of smoke production increased, a stable smoke layer formed under the inlets.

With exhaust inlets extended below the ceiling, the results indicated that the flow into the exhaust system was from both above and below the height of the inlet. In this case, there were tests in which the relative proportion of cold air to smoke was very high. Although this system was very inefficient, it was still effective in exhausting smoke.

## CONCLUSIONS

This paper presents results of physical model studies performed in an atrium space with mechanical exhaust. It also investigates the effect of fire size and opening location on the conditions in the atrium.

The results indicate that for the atrium studied, the correlations in NFPA 92B used for the design of exhaust system are valid. The results of these equations are consistent with the experimental findings. The results also demonstrate that when the exhaust systems operate near or just below their design capacity, they are effective in extracting gases from the hot layer without drawing in air from the lower layer. As expected, when the systems operate well above the required flow rates, fresh air from the lower layer enters the system. This, however, does not make the system ineffective as the level of the hot layer remains at acceptable levels.

The plugholing equation provided by Hinckley (1995) was investigated using the results of the various studies. A wide range of conditions were investigated. The results indicate that this correlation can be used to determine if a particular design will provide an efficient smoke exhaust system.

The physical model tests and numerical investigations indicate that it is very difficult to develop a test scenario in which the exhaust system would fail. With the rapid decrease in smoke production with decreasing clear height and the increasing efficiency of a smoke exhaust system as a smoke layer forms beneath the exhaust inlet, a stable, efficient system is generally obtained as the heat release rate increases.

## REFERENCES


BOCA. 1996. *The BOCA national building code*. Country Club Hills, Ill.: Building Officials and Code Administrators International Inc.

Cetegen, B.M., E.E. Zukowski, and T. Kubota. 1982. Entrainment and flame geometry of fire plumes, Ph.D. thesis of Cetegen, California Institute of Technology, Pasadena.

Cooper, L.Y., M. Harkleroad, J. Quintiere, and W. Rinkinen. 1982. An experimental study of upper hot layer stratification in full-scale multiroom fire scenarios. *Journal of Heat Transfer*, Vol. 104, pp. 741-749.

Hansell, G.O., and H.P. Morgan. 1994. Design approaches for smoke control in atrium buildings. BR-258. Garston, UK: Building Research Establishment.

Hadjisophocleous, G.V., G.D. Lougheed, C. McCartney, B.C. Taber, and S. Cao. 1998. Design approach for atrium exhaust effectiveness, ASHRAE RP-899. Ottawa, Ont: National Research Council of Canada.

Hadjisophocleous, G.V., G.D. Lougheed, and S. Cao. 1999. Numerical study of the effectiveness of atrium smoke exhaust systems. *ASHRAE Transactions* 105(1).

Heskestad, G. 1984. Engineering relations for fire plumes. *Fire Safety Journal*, Vol. 7, pp 25-32.

Hinckley, P.L. 1995. Smoke and heat venting. *SFPE Handbook of Fire Protection Engineering*. pp. 3-160-3-173. Quincy: National Fire Protection Association.

ICBO. 1994. *The uniform building code*. Whittier, Calif.: International Conference of Building Officials.

Klote, J.H. 1994. Method of predicting smoke movement in atria with application to smoke management. NISTIR 5516. Gaithersburg, Md.: National Institute of Standards and Technology.

Klote, J.H., and J.A. Milke. 1992. *Design of smoke management systems*. Atlanta: American Society of Heating, Refrigerating and Air-Conditioning Engineers, Inc.

Lougheed, G.D., and G.V. Hadjisophocleous. 1997. Investigation of atrium smoke exhaust effectiveness. *ASHRAE Transactions* 103: 1-15

McCaffrey, B.J. 1983. Momentum implications for buoyant diffusion flames. *Combustion and Flame*, 52: 149-167.

Morgan, H.P., and J.P. Gardiner. 1990. *Design principles for smoke ventilation in enclosed shopping centers*. BR186. Garston, U.K.: Building Research Establishment.

NFPA. 1995. *NFPA 92B, Guide for Smoke management systems in malls, atria, and large areas*. Quincy, Mass.: National Fire Protection Association.

Peacock, R.D., and V. Babrauskas. 1991. Analyses of large-scale fire test data. *Fire Safety Journal*, Vol. 17, pp 387-414.

Spratt, D., and A.J.M. Heselden. 1974. Efficient extraction of smoke from a thin layer under a ceiling. *Fire Research Note No. 1001*. U.K. Joint Fire Research Organization.

Yamana, T., and T. Tanaka. 1985. Smoke control in large spaces, Part 2: Smoke control experiments in a large scale space. *Fire Science*, Vol. 5, pp 41-54.